**SANDIA REPORT**
SAND2016-
Unlimited Release
November 2016

# Correlation of Noise Signature to Pulsed Power Events at the HERMES III Accelerator

Barbara A. Lewis, Nathan R. Joseph, J. Diego Salazar

Prepared by
Sandia National Laboratories
Albuquerque, New Mexico 87185 and Livermore, California 94550

Sandia National Laboratories is a multi-mission laboratory managed and operated by Sandia Corporation, a wholly owned subsidiary of Lockheed Martin Corporation, for the U.S. Department of Energy's National Nuclear Security Administration under contract DE-AC04-94AL85000.



Sandia National Laboratories

Issued by Sandia National Laboratories, operated for the United States Department of Energy by Sandia Corporation.



Printed in the United States of America. This report has been reproduced directly from the best available copy.

Available to DOE and DOE contractors from
U.S. Department of Energy
Office of Scientific and Technical Information
P.O. Box 62
Oak Ridge, TN 37831

Telephone: (865) 576-8401
Facsimile: (865) 576-5728
E-Mail: reports@osti.gov
Online ordering: http://www.osti.gov/scitech

Available to the public from
U.S. Department of Commerce
National Technical Information Service
5301 Shawnee Rd
Alexandria, VA 22312

Telephone: (800) 553-6847
Facsimile: (703) 605-6900
E-Mail: orders@ntis.gov
Online order: http://www.ntis.gov/search

SAND2016-12104
Unlimited Release
Printed November 2016

# Correlation of Noise Signature to Pulsed Power Events at the HERMES III Accelerator

Barbara A. Lewis, Nathan R. Joseph, J. Diego Salazar
AGT Accelerator Operations
Sandia National Laboratories
P.O. Box 5800
Albuquerque, New Mexico 87185-MS1106

**Abstract**

The HERMES III accelerator, which is located at Sandia National Laboratories' Tech Area IV, is the largest pulsed gamma X-ray source in the world. The accelerator is made up of 20 inductive cavities that are charged to 1 MV each by complex pulsed power circuitry. The firing time of the machine components ranges between the microsecond and nanosecond timescales. This results in a variety of electromagnetic frequencies when the accelerator fires. Testing was done to identify the HERMES electromagnetic noise signal and to map it to the various accelerator trigger events. This report will show the measurement methods used to capture the noise spectrum produced from the machine and correlate this noise signature with machine events.

# ACKNOWLEDGMENTS

The authors would like to thank the HERMES III team (Gary Tilley, Aaron Bowers, Ben Hughes, and John Lott – all from Org. 1342) for firing the accelerator and Roy Gutierrez, 5443, for lending us the dipole antenna.

# CONTENTS



# FIGURES

# NOMENCLATURE

| | |
|---|---|
| DAS | Data Acquisition System |
| EMI | Electromagnetic Interference |
| HERMES III | High-Energy Radiation Megavolt Electron Source III |
| MTA | Marx Trigger Amplifier |
| MITL | Magnetically Insulated Transmission Line |
| MTG | Marx Trigger Generator |
| IS | Intermediate Store Capacitor |
| PFL | Pulse Forming Line |
| SCD | Spherical Compton Diode |
| Scope | Digitizing oscilloscope |
| USR | User Screen Room |
| DOE | Department of Energy |
| SNL | Sandia National Laboratories |

# 1. INTRODUCTION

The HERMES III accelerator is made up of 10 Marx capacitor banks, each storing approximately 100 kJ of energy. Each Marx discharges into 2 intermediate store capacitors that each feed 4 pulse forming lines. Through this power conditioning process, the accelerator produces electromagnetic interference, or “noise” when the accelerator fires, due to switching of the various pulsed power components. The switching of the components compresses the electrical energy in time and space. The switching sequence starts on a microsecond timescale and compresses to a nanosecond timescale. Due to impedance mismatches among the different pulsed power components, electrical reflections occur. These reflections cause electromagnetic noise to be generated. Often customers are interested in the nominal noise signature of the accelerator to distinguish it from other EMI that may be measured.

EMI noise testing was conducted on HERMES III previously, but it was difficult to precisely tie the noise to accelerator events because a common timing for data acquisition was not in place. A common timing system was implemented at HERMES III in July 2015. With the common timing, all signals on the HERMES Data Acquisition System are referenced to a defined time zero. This makes it possible to compare times of signals on scopes with different triggers and in different locations of the accelerator.

## 1.1. Test Setup

An EMI enclosure (or “screen box”) was set up in the HERMES high bay. Two Tektronix 3054 scopes were put in the screen box, and a trigger was run from the User Screen Room to the scopes. Three loop antennas and a dipole antenna were mounted on the outside of the screen box. The antennas were approximately 5 feet west of the HERMES MITL center line, approximately 20 feet from the back of the accelerator. See Figure 1.

**Figure 1: Screen Box Location (Antennas Not Shown)**

Cables were connected from the antennas to the scopes inside of the screen box. Each antenna was teed so that its signal would go to one channel of each scope. One scope had each channel set on a more sensitive (smaller volts per division) setting in order to detect smaller signals. The MTA signal was connected to one channel in the EMI screen box to act as a timing fiducial.

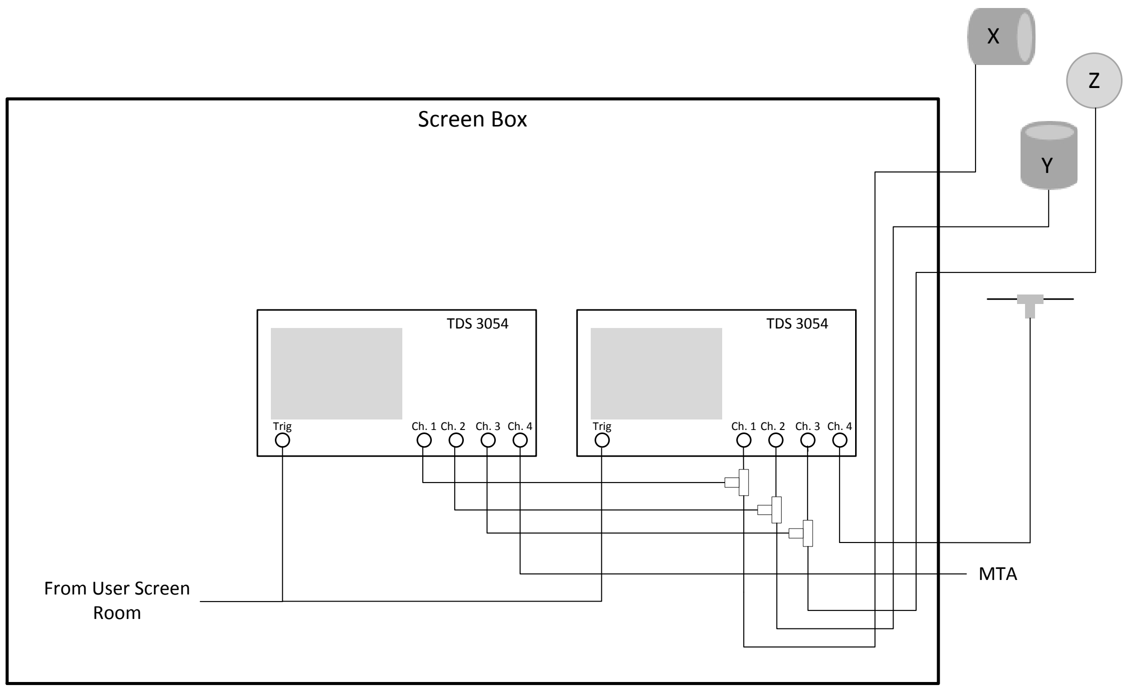


**Figure 2: Testing Configuration**

The scopes were time-tied to the main DAS using the following method:

- A cable of known length was run from the main DAS to the scope in the EMI screen box.
- A trigger source was connected to a scope in the EMI screen box and also to a scope in the main DAS.
- The header was set up with both scopes, accounting for cable length.
- The signal was sent to both scopes while triggering the system.
- The time difference between the signals was obtained.
- The time difference was entered into the time of fire column of the header for the signals on the EMI screen box scopes.

## 1.2. Measurement Methodology

The power flow through the HERMES III pulsed power components is as follows (see Figure 3):

MTA⇨MTG⇨Marx⇨IS⇨PFL⇨Cavity

To help distinguish noise signatures, the first two trigger systems were tested individually. Once the MTA and MTG signatures were produced, a full accelerator shot was conducted. The noise signature data is referenced in the time domain to correlate to machine events (i.e., the firing of machine components).

The MTA and MTG signatures can be isolated because individual MTA and MTG trigger tests were performed. The Marx signature can be isolated from the intermediate store signature because of the significant time difference between the firing of the Marxes and the firing of the rimfire switches (approximately a microsecond). The rest of the machine component signatures cannot be isolated because the remainder of the triggering sequence occurs automatically and in quick succession (within 400 nanoseconds), and the noise is dominated by the ringing of the intermediate stores.

The measurements taken from the various antennas are used only in a qualitative fashion and cannot be used quantitatively to infer field intensity.

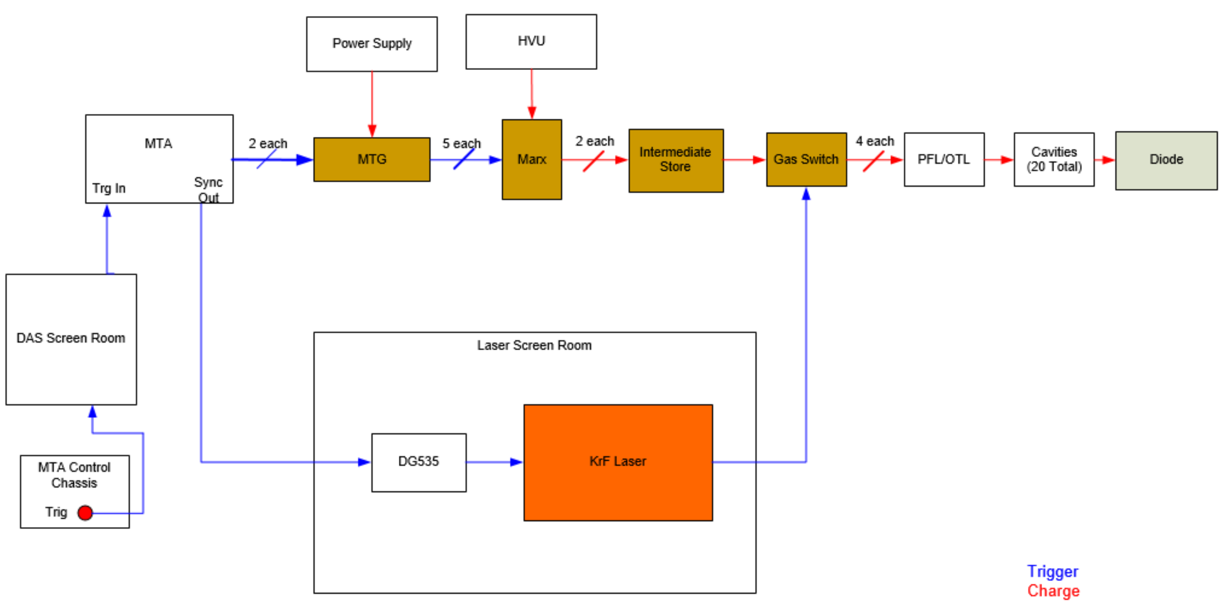


Figure 3: HERMES III Machine Triggering

# 2. RESULTS

## 2.1. MTA Only Trigger Test

The first trigger test was done firing only the MTA. On the scope channel with a small volts per division setting, a small amount of noise was visible. While there is a small spike at the onset of the MTA signal, the majority of the noise starts approximately 500 ns after the initial MTA signal. This indicates that the noise is generated as the trigger arrives at the MTGs, accounting for cable delay.

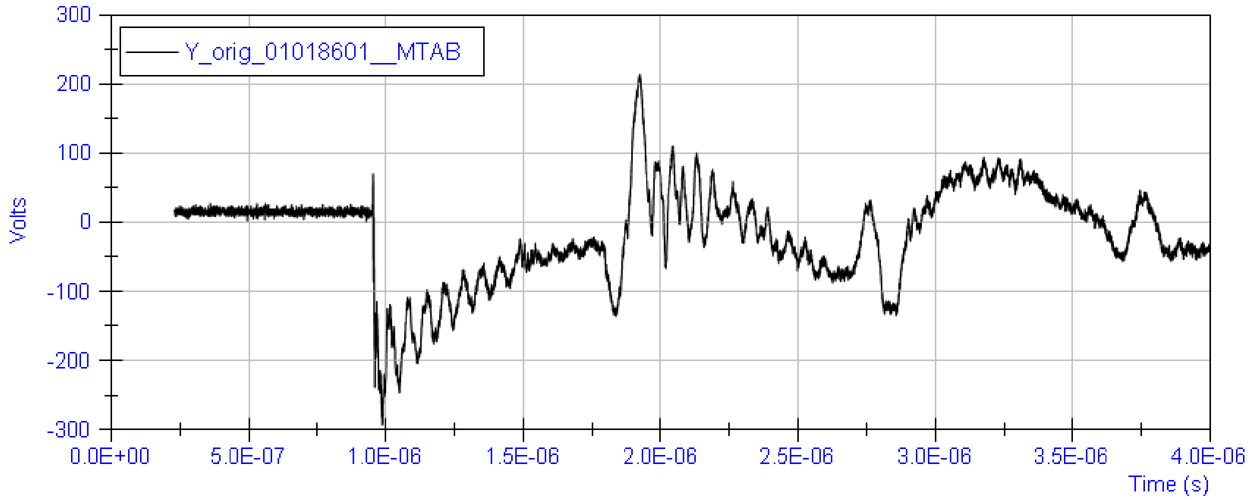


**Figure 4: MTA Signal**

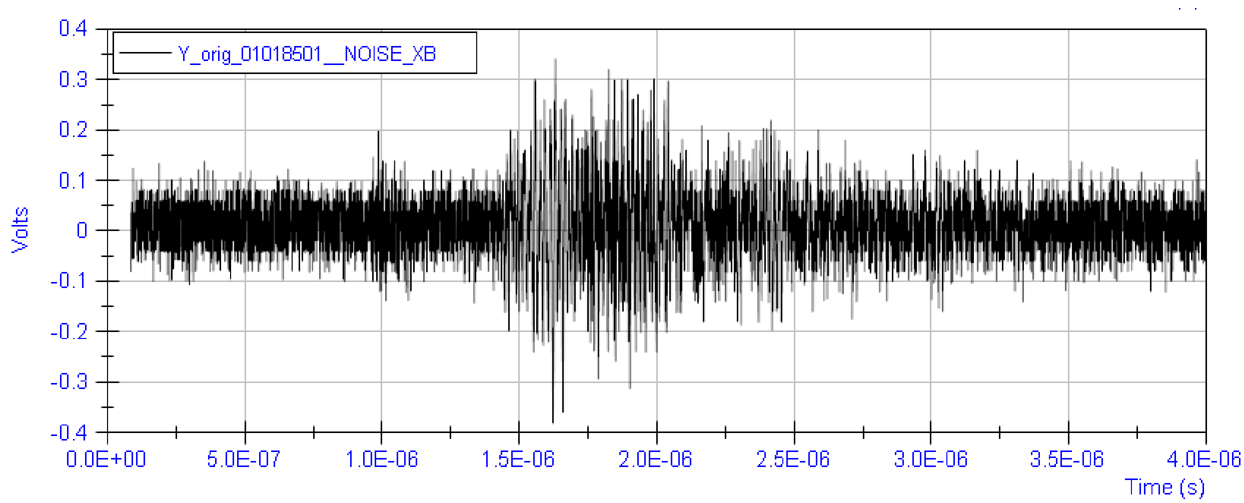


**Figure 5: Noise Signal on MTA Only Shot**

## 2.2. MTA and MTG Trigger Test

The next trigger test was done firing only the MTA and MTGs. The noise was an order of magnitude higher than with just the MTA. The noise from the MTA is also visible (see Figure 8).

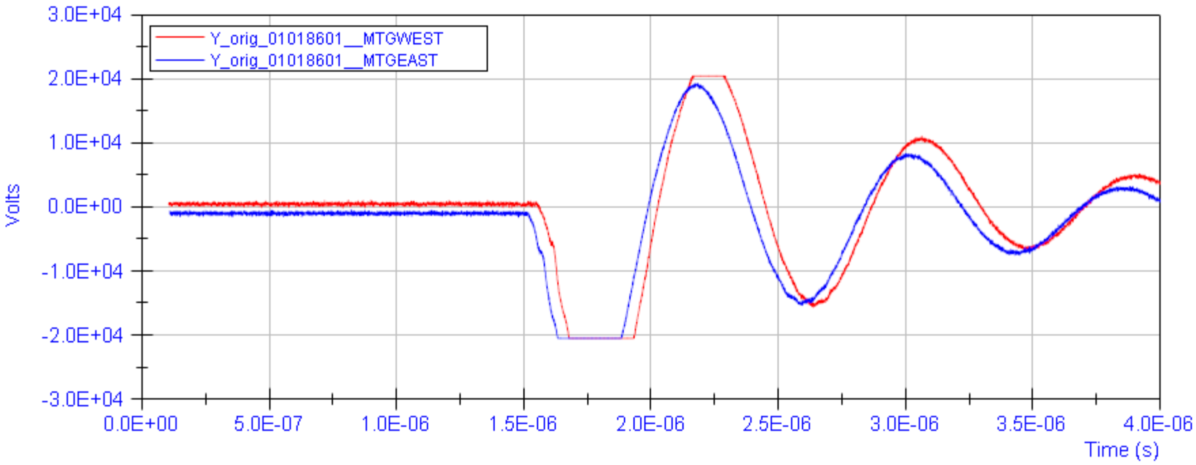


**Figure 6: MTG Signals**

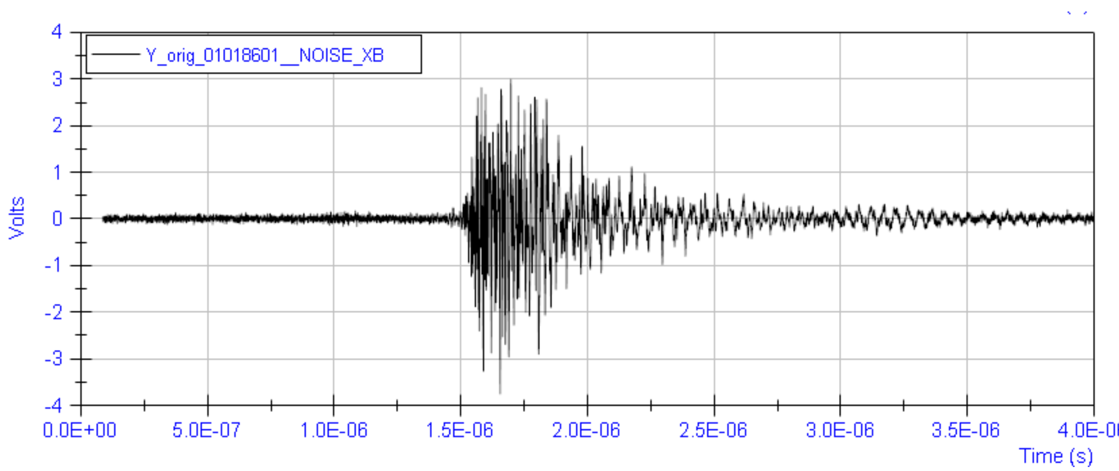


**Figure 7: Noise Signal**

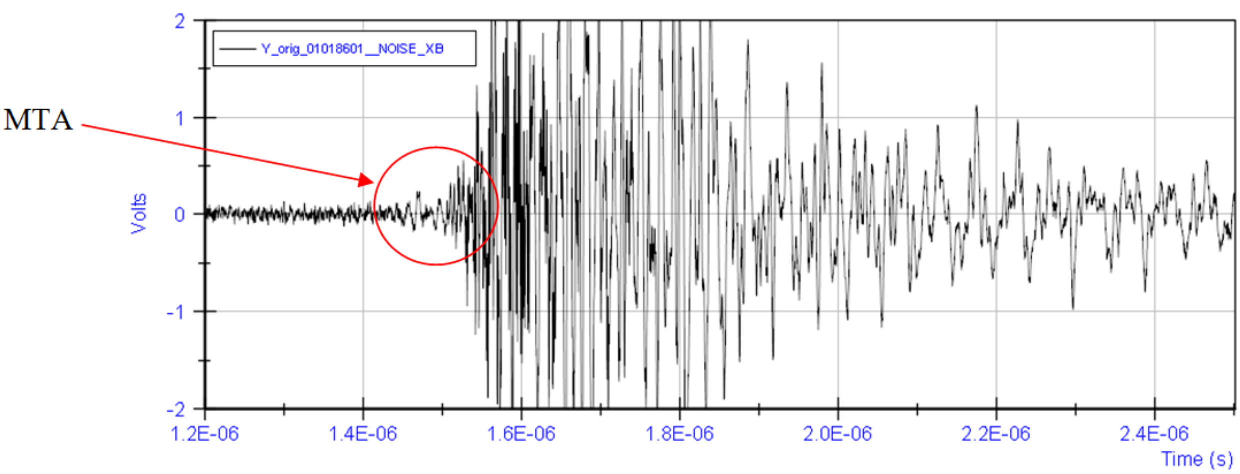


**Figure 8: Noise Signal, Zoomed In**

## 2.3. Full Accelerator Shot

The noise was measured on several full accelerator shots. The noise in the X, Y, and Z directions was measured by orienting the three loop antennas accordingly. On the smaller vertical scale (Figure 9), the MTA and MTG noise can be seen before the Marx noise dominates. On the larger scale (Figure 10), the noise from the MTGs can just be seen; however, the noise from the MTA is not visible on this scale.

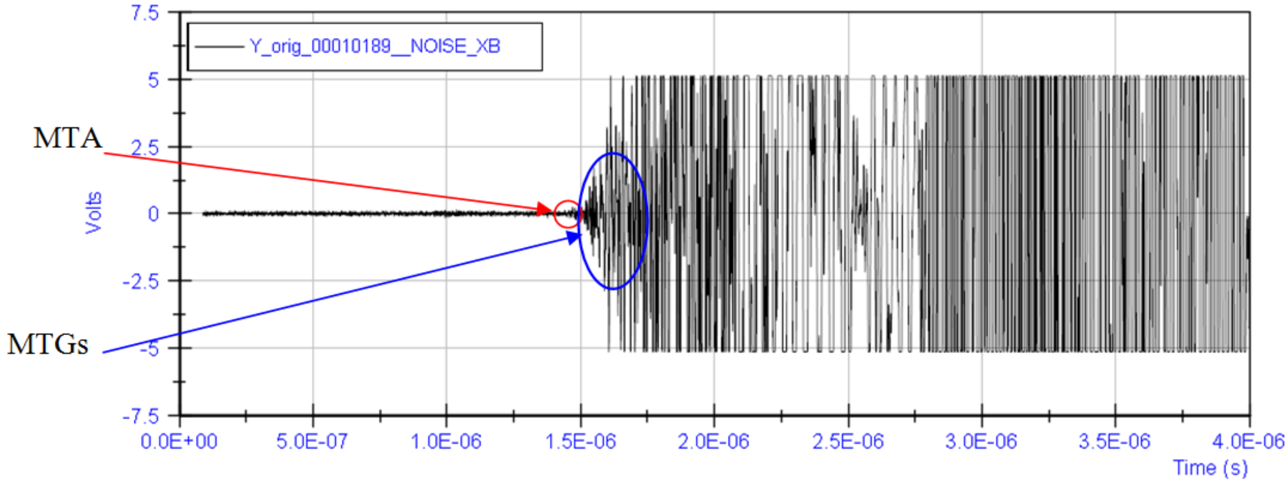


**Figure 9: Accelerator, Small Volts/Division Setting**

The majority of the noise from approximately 1.75E-6 s to approximately 2.75E-6 is due to the firing of the Marxes; the intermediate store capacitors are charging during this time but are not triggered until approximately 2.75E-6 s.

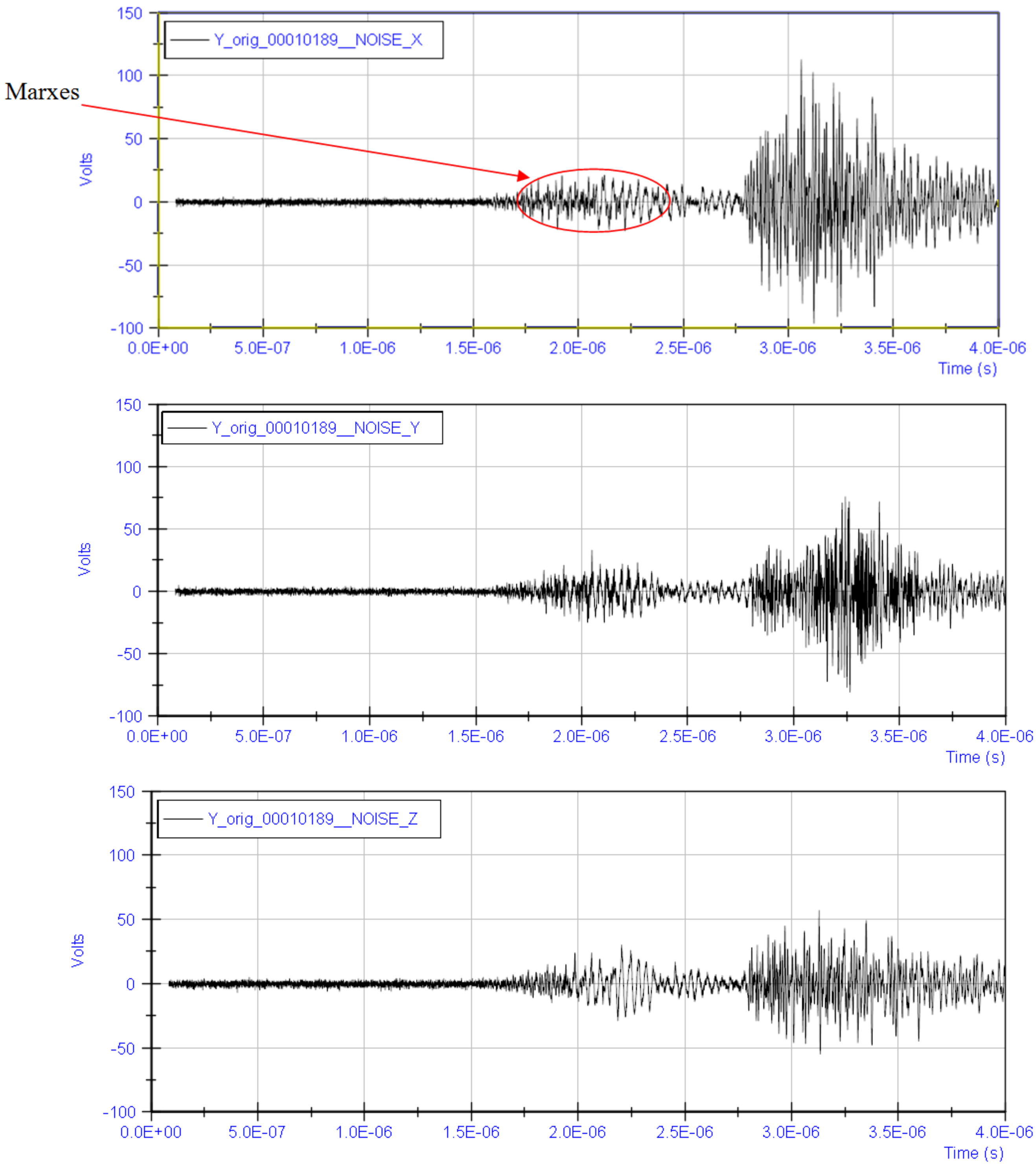


**Figure 10: Accelerator Shot – X, Y, and Z Axes**

The major machine events were plotted together by normalizing the vertical values so that they would fit on the same scale; see Figure 11. The first major noise starts to come up as the Marxes start discharging, about 1.75E-6 s. The noise diminishes until the intermediate stores fire, about 2.8E-6 s. The spherical Compton diode (SCD) signal represents the time of the output radiation pulse.

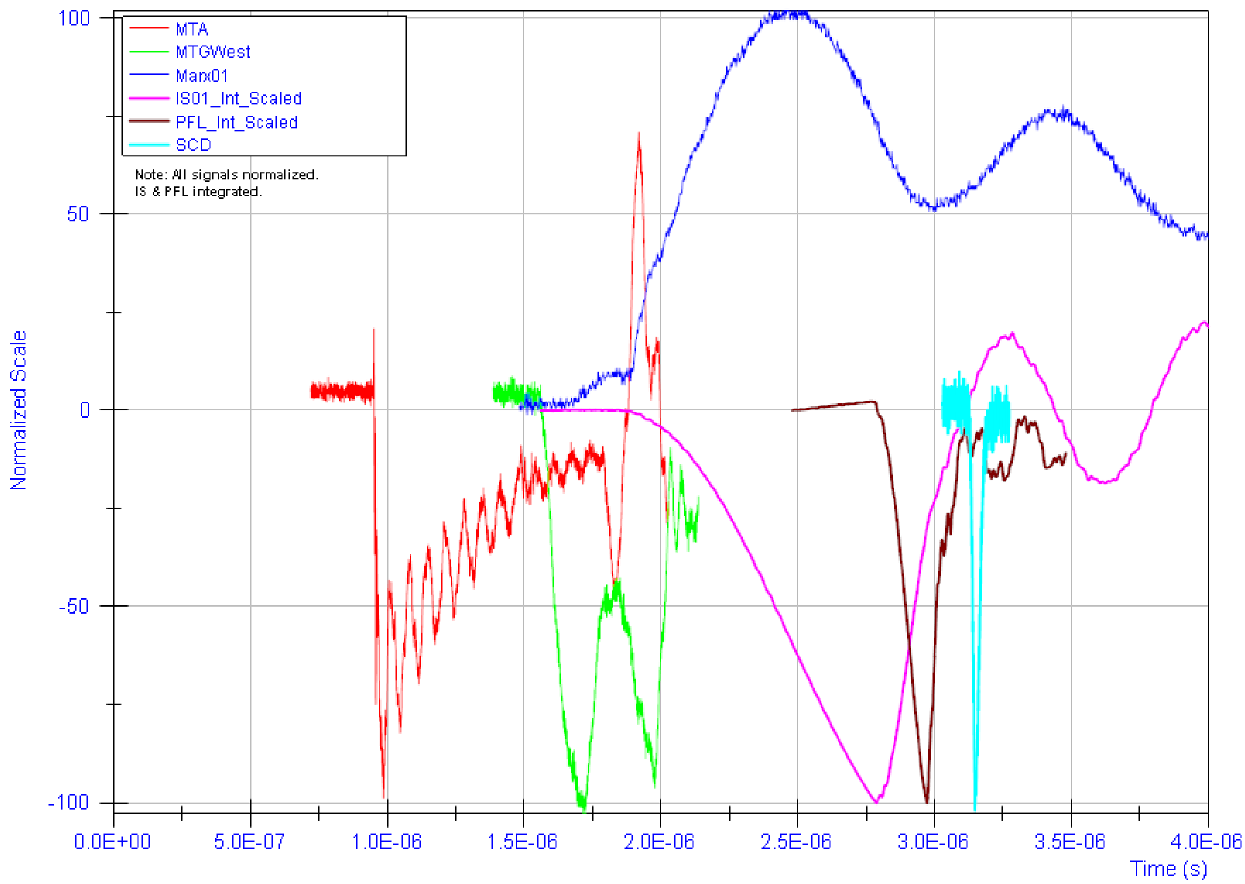


**Figure 11: Normalized HERMES III Accelerator Signals**

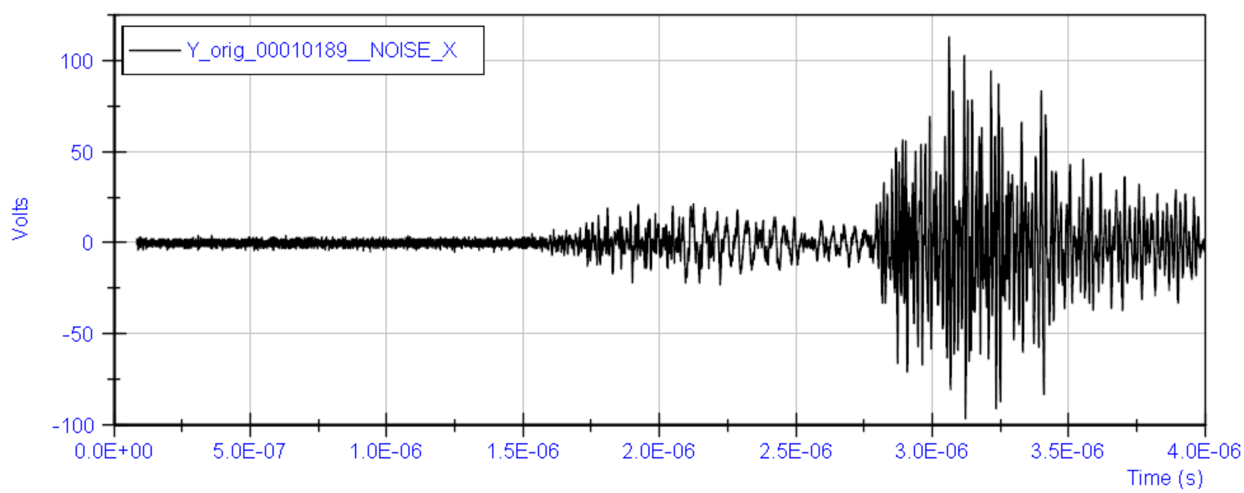


**Figure 12: Noise Signal from HERMES III Accelerator Shot**

Shot 10185 produced very little radiation due to the prefiring of the laser. Zooming in and comparing the noise waveform from shot 10185 with that from shot 10189 shows variations in the signals, but little difference in the Y and Z directions at the time of radiation output (3.13E-6 s); see Figure 13. There is more of a difference in the X direction, but the highest spike is slightly before radiation (3.06E-6). Some differences could be due to shot to shot variation. More testing is needed to determine if any of the noise signal is due to the radiation pulse.

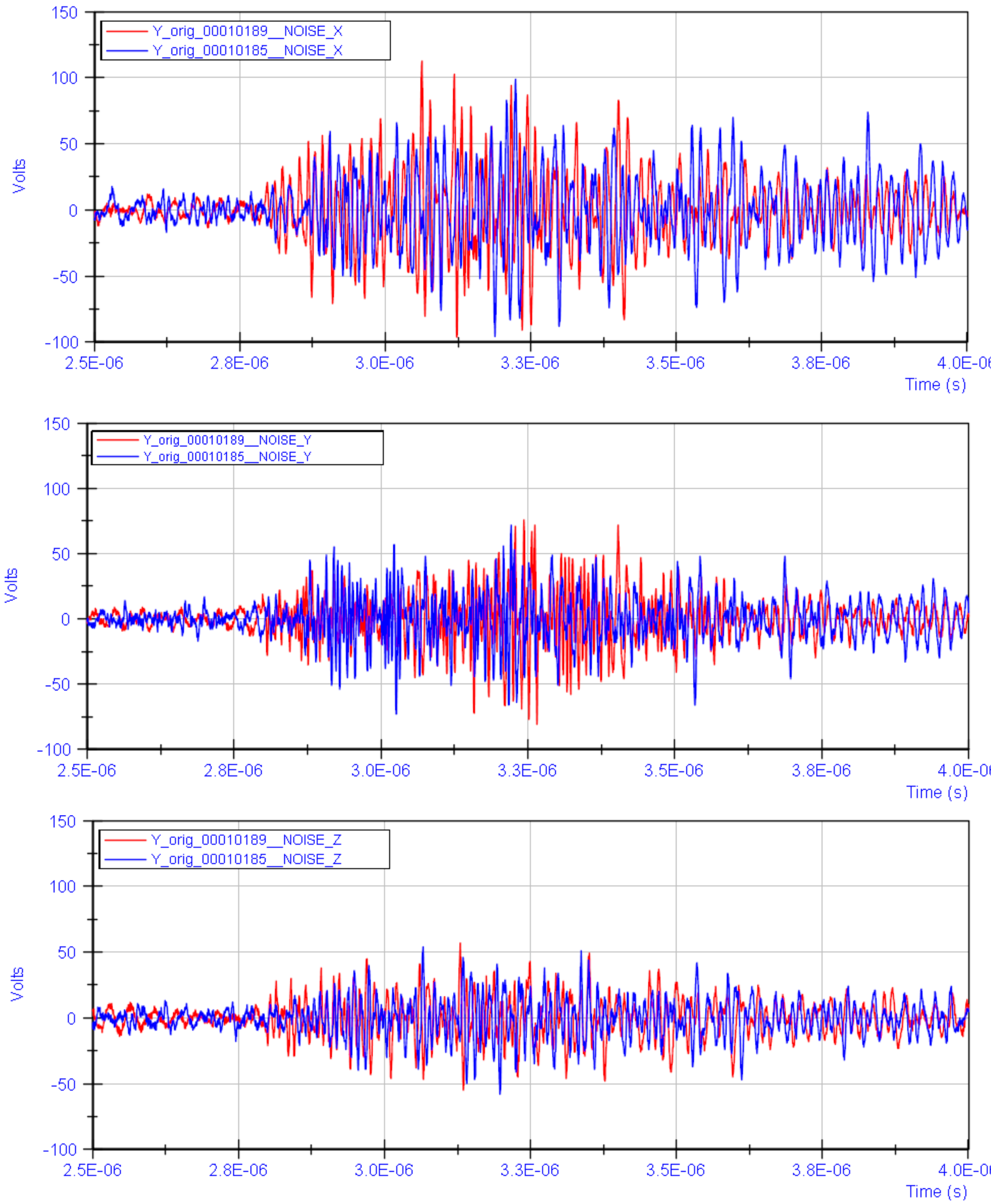


**Figure 13: Comparison of Radiation-Producing Shot (10189) with Low Radiation-Producing Shot (10185)**

## 2.4. Dipole Antenna

The dipole antenna has a similar signal as the loop antennas. See Figure 14. Because there was just one dipole antenna used, the axis of the dipole antenna was changed on different shots to allow a comparison between the loop antennas and the dipole antenna. See Figure 15, 16, and 17. On the dipole antenna, there is not much noise between the Marx noise and the Intermediate Store noise. This may be due to the different frequency response of each antenna type; further investigation is needed to determine the cause of the difference.

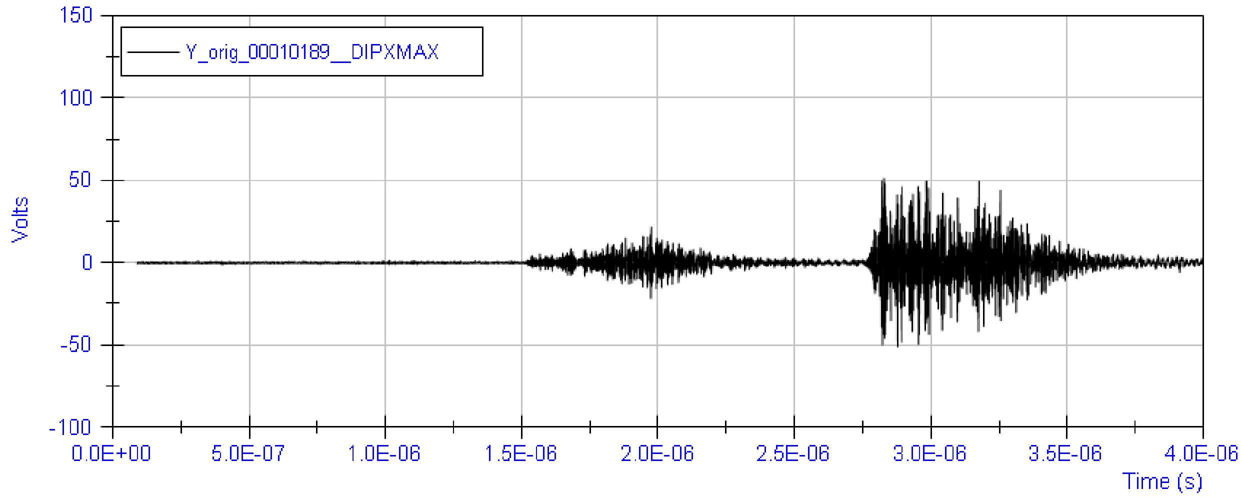


**Figure 14: Dipole Antenna (X Axis)**

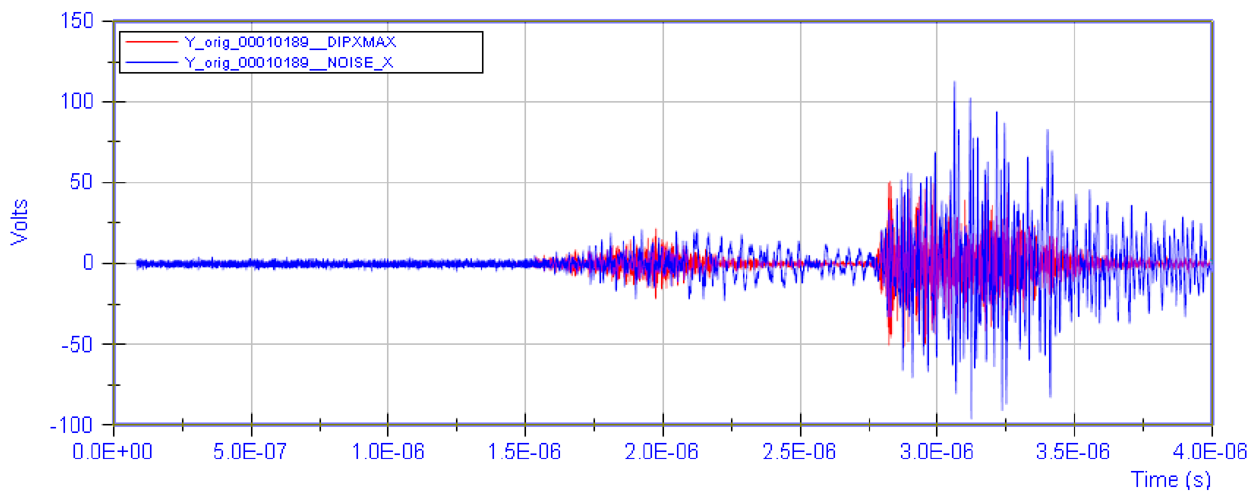


**Figure 15: Comparing Loop Antenna and Dipole Antenna (X Axis)**

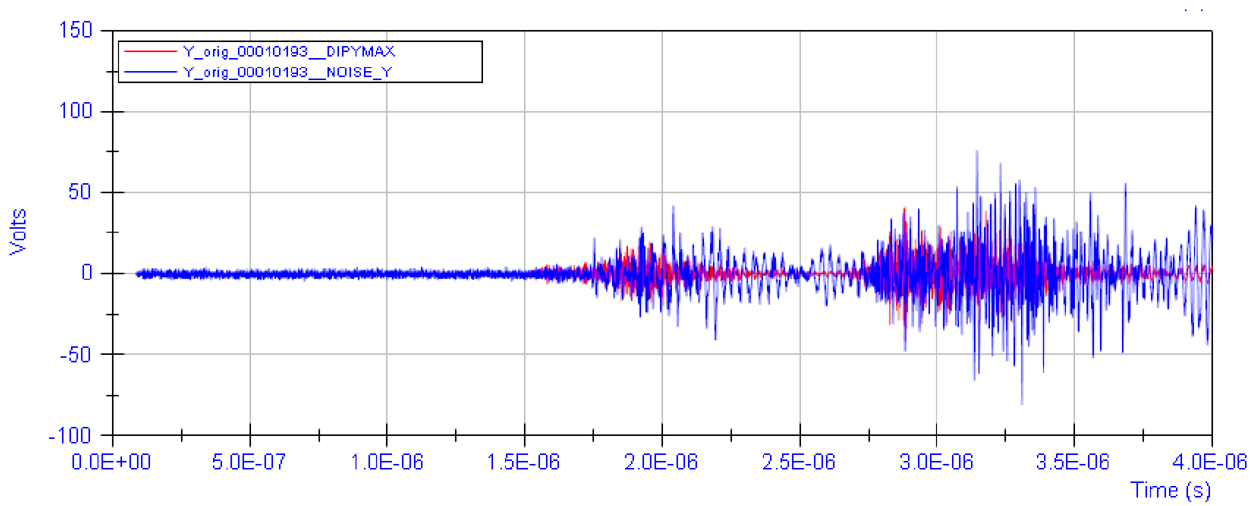


**Figure 16: Comparing Loop Antenna and Dipole Antenna (Y Axis)**

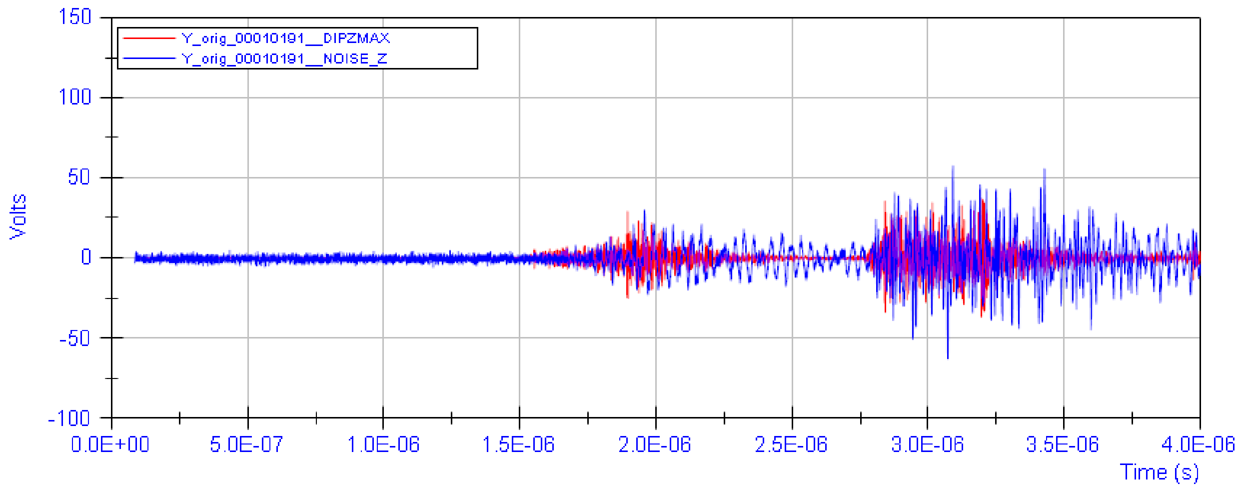


**Figure 17: Comparing Loop Antenna and Dipole Antenna (Z Axis)**

# 3. CONCLUSIONS

Each individual component of the HERMES III accelerator contributes to the overall noise signature. The noise signals from a low radiation-producing shot showed no distinguishable difference from a high radiation-producing shot at the testing location.

The electromagnetic noise signal is important to recognize so that it can be distinguished from other noise signals and so that it can provide useful information regarding the shielding needs for sensitive electronic devices.

Further testing and characterization is needed in order to make quantifiable measurements of the HERMES III electromagnetic spectrum. Additional testing locations will allow comparisons of the noise signature at each location around the accelerator.

Distribution

| | | | |
|---|---|---|---|
| 1 | MS1106 | Debra Kirschner | 1342 |
| 1 | MS1106 | Nathan Joseph | 1342 |
| 1 | MS1167 | Bryan Oliver | 1340 (electronic copy) |
| 1 | MS0899 | Technical Library | 9536 (electronic copy) |

Sandia National Laboratories